

## Practical Considerations for the Conceptual Design of an sCO<sub>2</sub> Cycle

Aaron McClung, Ph.D., Manager – R&D, [aaron.mclung@swri.org](mailto:aaron.mclung@swri.org)

Natalie Smith, Ph.D., Research Engineer, [natalie.smith@swri.org](mailto:natalie.smith@swri.org)

Tim Allison, Ph.D., Manager – R&D, [tim.allison@swri.org](mailto:tim.allison@swri.org)

Brittany Tom, Research Engineer, [brittany.tom@swri.org](mailto:brittany.tom@swri.org)

Southwest Research Institute, San Antonio, TX



Dr. Aaron McClung is the manager of the Power Cycle Machinery Section at Southwest Research Institute® (SwRI®) in San Antonio, Texas. His research at SwRI includes optimization of Supercritical Carbon Dioxide (sCO<sub>2</sub>) power cycles, demonstration of sCO<sub>2</sub> systems and components, and the use of simulation to understand and optimize complex thermodynamic systems. Dr. McClung earned his Ph.D. in Aeronautical Engineering from the Air Force Institute of Technology.



Dr. Natalie Smith is a Research Engineer in the Rotating Machinery Dynamics Section at Southwest Research Institute in San Antonio, Texas. Her research experience at SwRI includes aerodynamic design, analysis, and testing of turbomachinery for various applications including power generation, oil and gas, and Supercritical Carbon Dioxide (sCO<sub>2</sub>). She earned her Ph.D. in Aeronautics and Astronautics from Purdue University.



Dr. Tim Allison is the manager for the Rotating Machinery Dynamics Section at Southwest Research Institute in San Antonio, Texas. His research at SwRI includes turbomachinery and test rig design, finite element analysis, modal testing, instrumentation, and performance testing for applications including centrifugal compressors, pumps, axial/radial expanders, gas turbines, reciprocating compressor valves, and test rigs for rotordynamics, blade dynamics, and aerodynamic performance. He earned his Ph.D. in Mechanical Engineering from Virginia Polytechnic Institute and State University and has authored over 50 technical papers related to machinery and piping systems and structures.



Brittany Tom is a Research Engineer in the Power Cycle Machinery Section at Southwest Research Institute in San Antonio, Texas. Mrs. Tom's research activities at Southwest Research Institute support the development and testing of high-pressure machinery for advanced power cycles. She is currently supporting the design of the 10MWe supercritical CO<sub>2</sub> pilot plant. She earned her bachelor of science degree in Aerospace Engineering from Massachusetts Institute of Technology.

### ABSTRACT

Supercritical Carbon Dioxide (sCO<sub>2</sub>) cycles are of interest for a wide range of applications with varying temperatures, scales, and performance requirements. This range of operational requirements translate to a wide variety of feasible power block designs, with interconnected design variables that include cycle type and operating conditions, materials selection, heat exchanger type, and turbomachinery details including speed, size, staging, axial/radial architecture, bearing/seal types, etc. These design variables often conflict with one another and result in tradeoffs in component performance and system layout when optimizing the overall sCO<sub>2</sub> system. This paper focuses on the conceptual turbomachinery design

and system layout for a notional 500 kW Recompression Closed Brayton cycle and presents a recommended approach for an sCO<sub>2</sub> power system conceptual design that incorporates efficient iteration of key design decisions including machinery sizing/staging/performance and component limits. Specific rules of thumb are provided for temperature thresholds and various machinery component performance limits.

## **INTRODUCTION**

The design of an optimized sCO<sub>2</sub> power cycle represents a compromise between competing design goals that consider the thermodynamic cycle, operating requirements, system architecture, machinery design, component selection, material selection, and pressure losses. This paper focuses on turbomachinery sizing and system architecture trades during the conceptual design of a 500 kW sCO<sub>2</sub> Recompression Closed Brayton Cycle (RCBC) system and outlines an approach for sCO<sub>2</sub> power system conceptual design that incorporates efficient iteration of key design decisions including cycle optimization, machinery sizing, staging, and performance, component limits, and system off-design performance. A 500 kW RCBC system was selected for this notional exercise because the RCBC is a common high thermodynamic efficiency closed Brayton cycle discussed in literature and the 500 kW power level highlights critical system trades that must be considered during turbomachinery design.

### **Design Process**

The general design process for a sCO<sub>2</sub> power system progresses in multiple stages that start with conceptual system design and conceptual component design progressing through detail component and system design. Conceptual system design includes the identification of relevant thermodynamic cycle configurations and initial cycle design point optimization of those cycles to determine overall system performance and component operating conditions. The component efficiencies used in the thermodynamic simulation are based on the designers' experience or pulled from experience charts in literature such as Baljé charts for turbomachinery [Baljé, 1981]. The thermodynamic analysis provides system efficiencies and state points which are used as boundary conditions for the initial component design and selection. Several iterations may be completed where the 0-D component performance estimates are revised until a preferred set of cycles and machinery configurations are selected to progress through conceptual component design and layout of the mechanical system.

Conceptual component design uses the thermodynamic state points and desired efficiency boundary conditions and design objectives to advance the turbomachinery through 1-D design to establish the physical system characteristics such as staging, hub and shroud diameters and revise component performance estimates. The physical dimensions are fed into the system mechanical layout while the revised performance estimates and component operating maps are fed back into a revised cycle analysis to compute off design performance for the conceptual design. Figure 1 illustrates this iterative process.

Detail system design extends the 1-D component design through a complete system design including turbomachinery mechanical design, final system layout, piping system design, and controls system development. The remainder of this paper focuses on the conceptual design and mechanical layout of a notional 500 kW sCO<sub>2</sub> power block.

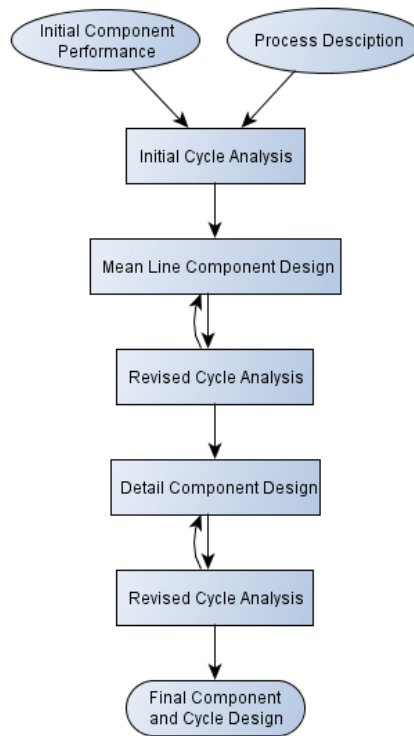


**Figure 1. Simplified Design Process**

## **THERMODYNAMIC DESIGN**

Conceptual design of a sCO<sub>2</sub> cycle for a commercial application includes thermodynamic cycle selection and optimization that factor the type of the sCO<sub>2</sub> system such as primary power generation or waste heat recovery, the desired power output, the integrated heat source such as a gas turbine exhaust gas stream, nuclear reactor, concentrating solar power, or a fired heater, and the local ambient conditions and other local constraints such as space available and availability of water for cooling.

To present the conceptual turbomachinery and system layout design process in an open manner, a 500 kW RCBC system was selected for this notional exercise because the RCBC is a common high thermodynamic efficiency closed Brayton cycle discussed in literature and the 500 kW power level highlights critical system trades that must be considered during turbomachinery design. This cycle, shown in Figure 2, utilizes a flow split and a hot bypass compressor (also referenced as a recompressor) to maximize thermodynamic efficiency. The use of a flow split and hot bypass compressor allows the cycle to avoid a pinch point in the low temperature recuperator, maximizing the recuperation of thermal energy between the hot turbine exhaust and the cold compressor discharge. This cycle is the current benchmark cycle for high efficiency sCO<sub>2</sub> cycles being considered for Concentrating Solar Power (CSP) and Nuclear applications.

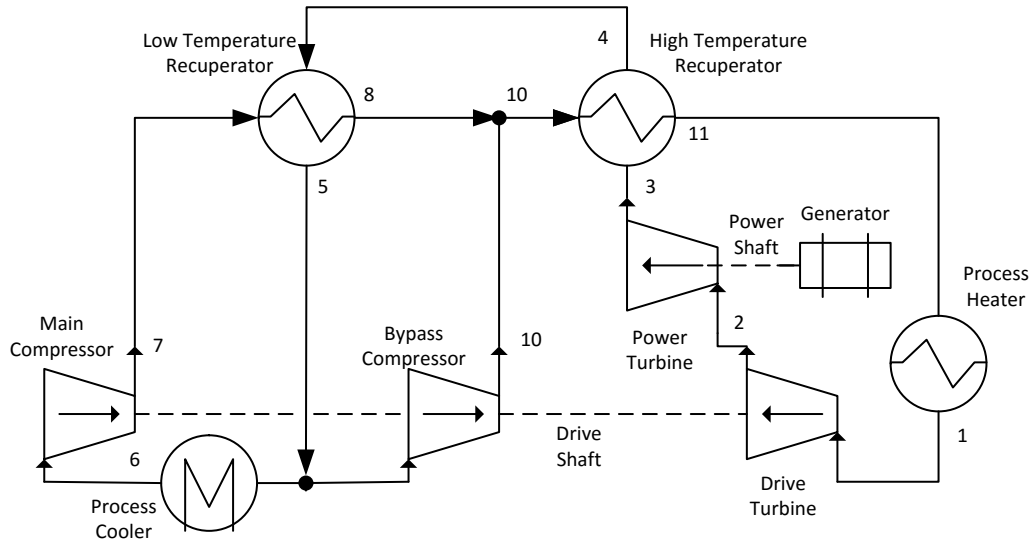


Figure 2 Dual-Shaft Recompression Closed Brayton Cycle (RCBC) flow diagram with Drive and Power Turbines in series. The RCBC cycle uses a hot bypass compressor and a low temperature recuperator to avoid a pinch point in the system recuperation.

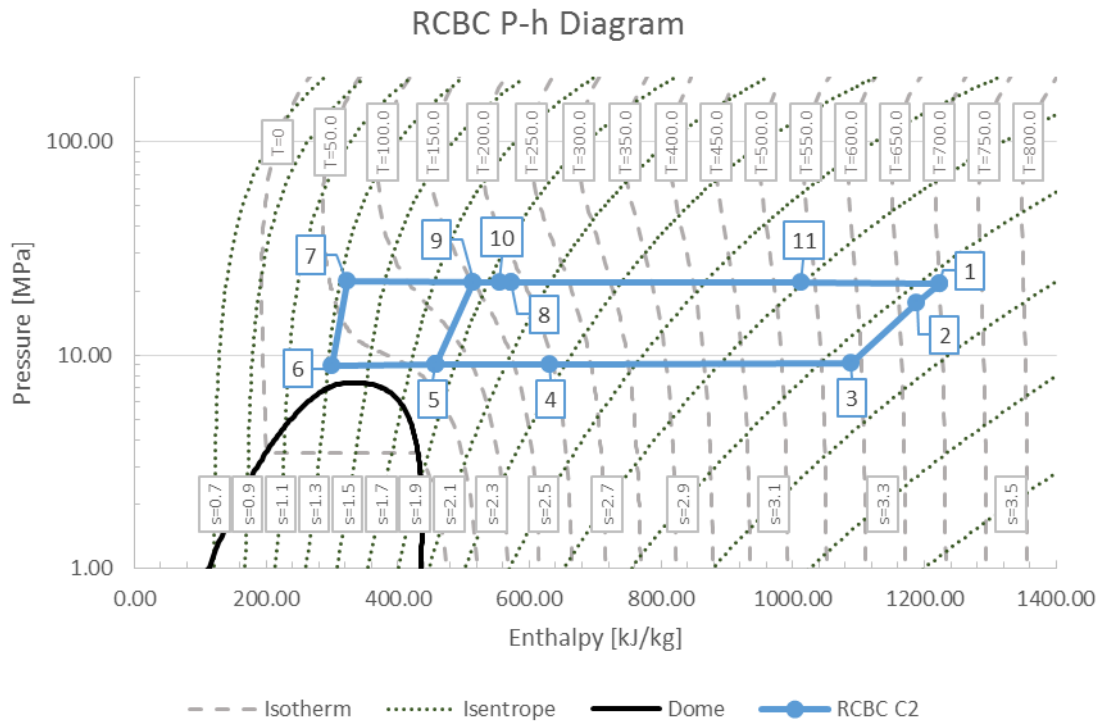


Figure 3. Recompression Closed Brayton Cycle (RCBC) Pressure-Enthalpy Diagram. System components include the Drive Turbine (1 -> 2), Power Turbine (2 -> 3), High Temperature Recuperator (Low P) (3 -> 4), Low Temperature Recuperator (Low P) (4 -> 5), Flow Split (5), Process Cooler (5 -> 6), Main Compressor (6 -> 7), Low Temperature Recuperator (High P) (7 -> 8), Bypass Compressor (5 -> 9), Flow Mix (8 + 5 -> 10), High Temperature Recuperator (High P) (10 -> 11), and Primary Heater Interface (11 -> 1)

## Conceptual Design

A set of cycle design point solutions were computed using Numerical Propulsion System Simulation (NPSS) to estimate thermodynamic performance of the notional 500 kW RCBC system and determine the specific component operating conditions. The model used experience based component performance estimates for the Turbine, Main Compressor, Bypass Compressor, High Temperature Recuperator, Low Temperature Recuperator, pressure losses to account for heat exchangers and system piping, and mechanical losses to account for bearings, seals, and generators. Design conditions for the turbomachinery and overall cycle performance are shown in Table 1 for four different cycle cases (difference overall and component efficiencies) presented in this paper.

**Table 1. Component operating conditions and RCBC cycle performance for selected cases. Cycle efficiency represents the cycle thermal efficiency based on shaft power, Power block efficiency represents thermal efficiency based on net electric power when factoring in auxiliary system loads , gearbox (as applicable), and generator losses.**

			Cycle Case			
			C1	C2	C3	C6
Main Compressor	Pt1	bar	89.00	89.00	89.00	89.00
	Tt1	C	34.98	34.98	34.98	34.98
	Pt2	bar	220.85	220.85	220.85	220.85
	W	kg/sec	4.91	4.48	4.44	5.32
	Isentropic Efficiency	%	65.00	80.00	85.00	64.00
Bypass Compressor	Pt1	bar	89.99	89.99	89.99	89.99
	Tt1	C	69.61	66.56	66.04	69.41
	Pt2	bar	219.53	219.53	219.53	219.53
	W	kg/sec	2.10	1.92	1.90	2.28
	Isentropic Efficiency	%	60.00	75.00	75.00	67.00
Drive Turbine	Pt1	bar	214.95	214.95	214.95	214.95
	Tt1	C	699.99	699.99	699.99	699.99
	Pt2	bar	166.16	175.44	176.58	165.49
	Tt2	C	664.98	672.26	673.14	666.59
	W	kg/sec	7.01	6.40	6.34	7.60
	Power	kW	296.00	215.00	206.00	306.00
	Isentropic Efficiency	%	87.50	87.50	87.50	82.00
Power Turbine	Pt1	bar	166.16	175.44	176.58	165.49
	Tt1	C	664.98	672.26	673.14	666.59
	Pt2	bar	91.26	91.26	91.26	91.26
	Tt2	C	587.23	587.21	587.20	594.76
	W	kg/sec	7.01	6.40	6.34	7.60
	Power	kW	643.00	643.00	643.00	643.00
	Isentropic Efficiency	%	88.50	88.50	88.50	82.00
Cycle	Thermal Efficiency	%	44.60	47.80	48.20	42.60
	Shaft Power	kW	643.00	643.00	643.00	643.00
	Thermal Input	kW	1442.94	1346.19	1334.26	1508.16
Power Block	Thermal Efficiency	%	34.70	37.10	37.50	33.20
	Net Power	kW	500.00	500.00	500.00	500.00
	Thermal Input	kW	1442.94	1346.19	1334.26	1508.16
	Mechanical Losses	%	22.24	22.24	22.24	22.24

The inlet temperature for the Main Compressor was set to 35 °C based on estimated average cooling temperature plus a reasonable approach temperature in the cooler. This temperature is also selected to avoid operation of the main compressor across a liquid-supercritical transition. Although operating in this regime may be permissible, the density gradients across this transition region may lead to flow

stratification near the compressor inlet and introduce additional uncertainty in expected compressor performance and mechanical reliability.

Even above the critical temperature, high Mach numbers at the compressor inlet can cause local static pressure and temperature drop, leading to condensation or cavitation at the inlet. The isenthalpic pressure margin to cavitation/condensation at inlet static conditions was calculated as a function of Mach number and inlet total pressure at 35 °C and is shown in Figure 4. The results show that, at the selected inlet pressure of 9 MPa, a 2-3 MPa margin to phase change exists for an inlet Mach number up to 0.25, which is considered to be a reasonable value based on reference designs.

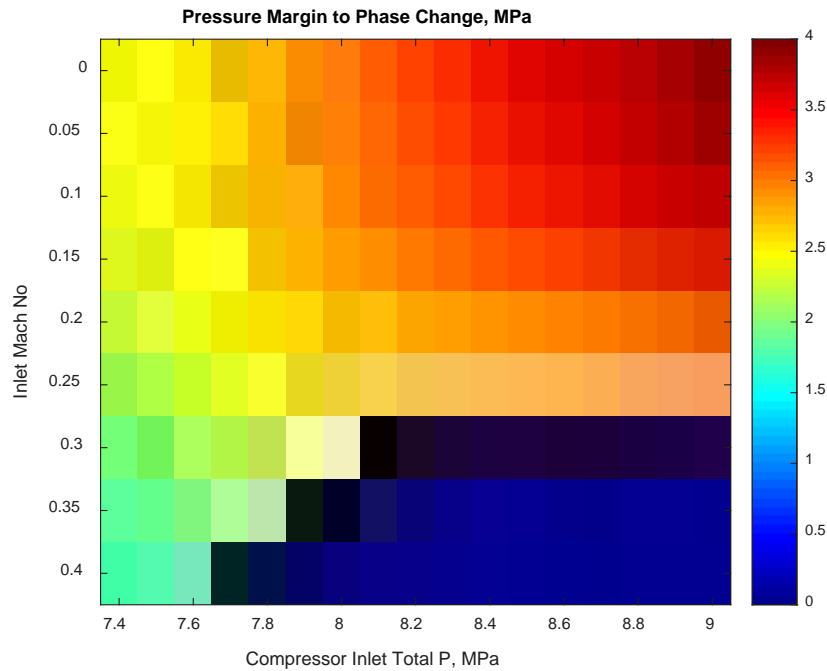


Figure 4. Pressure Margin to Condensation for a 35 C Compressor Inlet Temperature

## AERODYNAMIC DESIGN

At the conceptual design phase, turbomachinery component aerodynamic design consists of thermodynamic analysis coupled with experience-based trends to provide initial sizing and performance metrics. Temperatures, pressures, mass flow rate, and power requirements from the cycle feed into required inputs to the aerodynamic design of the compressors and turbine(s). This section consists of the turbomachinery design methodology and design metric sweeps utilized to evaluate configuration options for each of the cycle cases outlined in Table 1. Based on cycle conditions, required component power splits were determined. The net power,  $P_{net}$ , from the cycle was defined as

$$P_{net} = \eta_{gen} [\eta_{mech,T} P_T - (P_C + P_{BC}) / \eta_{mech,C}] - P_{H2Opump}$$

where  $P_T$ ,  $P_C$ ,  $P_{RBC}$ ,  $P_{blower}$ , and  $P_{H2Opump}$  are the power associated with the turbine, compressor, bypass compressor, and cooling water pump, respectively, and  $\eta_{gen}$ ,  $\eta_{mech,T}$ , and  $\eta_{mech,C}$  are generator efficiency (94%), turbine mechanical efficiency (96%), and compressor mechanical efficiency (96%), respectively. The initial efficiencies used here are based on experience and design intent; these values are updated in subsequent cycle analysis and aerodynamic sizing iterations.

## Compressor Conceptual Design

Initial conceptual sizing of the Main Compressor and Bypass Compressor were completed using an in-house SwRI sizing code based on Baljé [1981] approximations and Aungier comparisons [2000]. Figure 5 depicts the basic conceptual compressor design process, also used by Bidkar et al. [2016] in the design of sCO<sub>2</sub> compressors for 50MWe and 450MWe sCO<sub>2</sub> systems. The sizing inputs include thermodynamic conditions provided by the cycle analysis, rotational speed, number of stages, and stage inlet Mach number. For sCO<sub>2</sub> applications with Main Compressor inlet conditions operating very close to the dome, inlet Mach number must be carefully considered to avoid phase change as discussed in the previous section. This design method utilizes specific speed ( $n_s$ ) and specific diameter ( $d_s$ ) correlated to peak efficiency trend on the Baljé chart to estimate efficiency and impeller diameter. An example Baljé compressor chart is shown in Figure 6. In addition to the parameters shown in Figure 5, design experience from the literature [Rohlik, 1968] provides estimations for inlet shroud diameter to exit diameter ratio, potential limitations on casing or hub diameters, and desired inlet Mach number which provide sufficient information to calculate inlet hub and shroud diameters. Real gas assumptions are used when computing thermodynamic properties using REFPROP [Lemmon et al., 2013]. This process is repeated for each stage in a design.

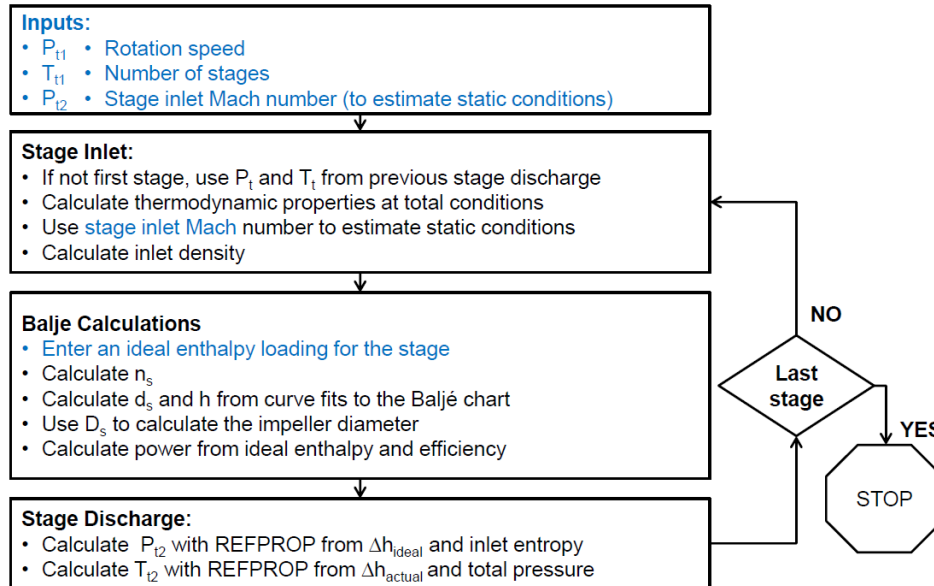


Figure 5. Flowchart of compressor sizing procedure for each stage of a multistage machine [Bidkar et al. 2016]

From the cycle requirements of pressure and temperature at the inlet and exit and an inlet Mach number to avoid cavitation, sweeps of compressor sizing were completed over an array of rotational speeds from 30,000 to 180,000 rpm for machines with one to five stages. These design point parameter sweeps for the compressor and bypass compressor result in efficiency and machine sizing (diameters) shown in Figure 7 for the cycle case 2, similar results were acquired for the other cycle cases, but are not presented in detail here. For all cycle cases considered, the peak efficiency operating range for the compressors was at high speeds, in excess of 160,000 rpm expect for high-stage count main compressor designs, similar to the results shown for cycle case 2. As stage count increases, peak efficiency rotational speed decreases, though, in general, stage count will be kept as low as possible to reduce system complexity and cost. The results shown in Figure 7 motivate Main Compressor and Bypass Compressor designs which operate at high speeds in order to maximize efficiency. Practical rotational speed limits were considered (as

discussed further in the following section) while still maintaining as high of efficiency as possible. Also shown in Figure 7 are the sizing results (hub diameters and impeller diameters) for each speed and stage combination. Component limitations covered in the following section will use this information to ensure minimum hub diameters and maximum impeller diameter requirements are satisfied. Finally, two design choices have been highlighted in the Figure 7 which represent two high efficiency high speed configurations to facilitate discussion of layout selection.

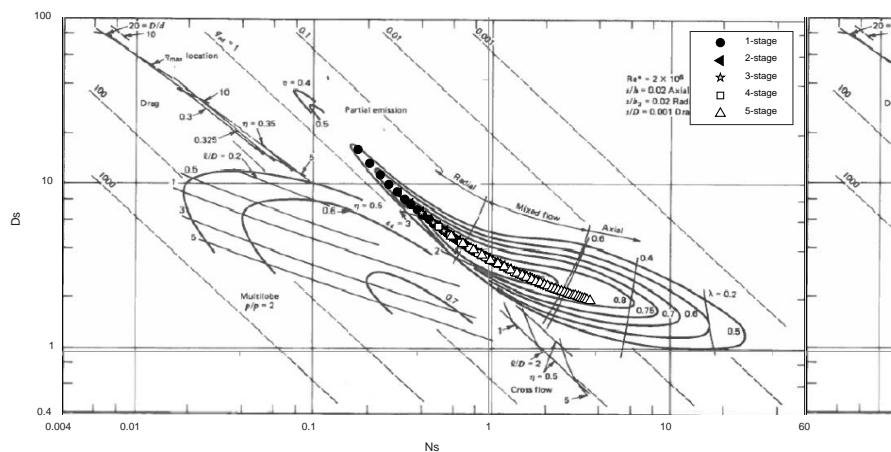
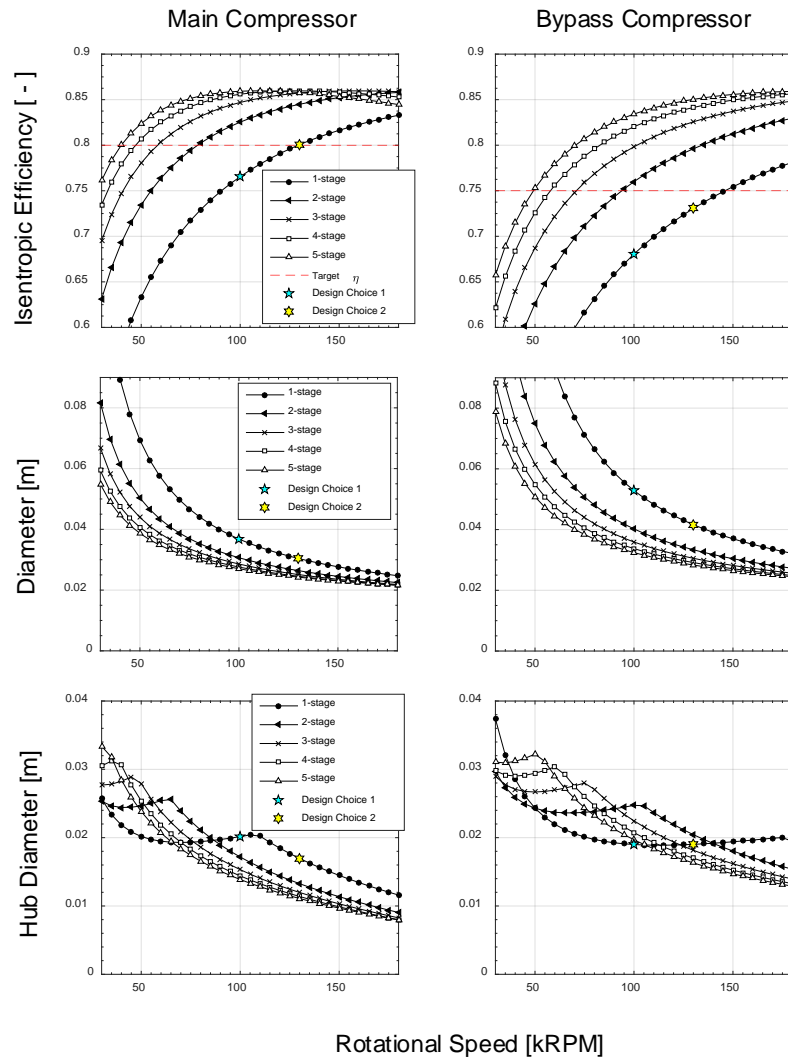


Figure 6. Baljé compressor chart with design sizing sweeps along peak efficiency [Adapted from Baljé, 1981]



**Figure 7. Compressor and bypass compressor efficiency and sizing results from design parameter sweeps for Cycle Case 2**

### Turbine Conceptual Design

The compressor and turbine conceptual designs use a similar methodology, but utilize different tools. The turbine conceptual design was completed using historical data and Baljé approximations relating to specific speed, specific diameter, and efficiency. Moreover, the radial turbine design sizing code developed by NASA (RTD) [NASA] was used. The code uses ideal gas assumptions in its calculations, but inlet and exit flow properties and turbine performance are verified with real gas calculations in REFPROP. Various losses accounted for in the 1-D turbine design include shroud and hub leakages, hub-side and shroud-side cavity windage loss, and total pressure losses from volute, nozzle vanes, diffuser, and return channel. These losses can reduce turbine efficiency by 3-6 points. Design point parameter sweeps included rotational speeds from 30,000 to 180,000 rpm and one to three stage machines.

The application at the 500 kW power level has unique design trades associated with turbomachinery performance and their component limitation. Therefore, several design configurations were evaluated to optimize turbomachinery performance and integration. Specifically, single- and split-shaft turbine configurations were evaluated. A split-shaft turbine configuration distributes the power generation

requirement between multiple machines. For the case discussed herein, one turbine (drive turbine) produces the power required to run the compressors, while a second turbine (power turbine) supplies the cycle output power. This can allow for increased flexibility with system architecture and/or machine performance optimized to different shaft speeds. Split-shaft design can be oriented in a parallel or series configuration. A parallel configuration would involve a flow split between the power and drive turbines and both machines would have the same enthalpy change. Alternatively, the turbines could be arranged in series where both run on the flow cycle mass flow, but the enthalpy change is split between them. Based on machinery limitations and an understanding of the sizing calculations, only series configurations were considered for the split-shaft configurations. This allowed for higher flow rates with lower power (enthalpy change) requirements per machine, thus reducing optimal operating speeds and required number of stages. For series configuration, the order of the two machines must also be chosen. In all cases, drive turbine before the power turbine resulted in small benefits in peak efficiency operating ranges for the machines.

The results from design point sweeps of a wide range of rotational speeds (30,000 to 180,000 rpm) and number of stages (one to three) provide the related efficiency and machine diameters. The results for the cycle case 2 are shown in Figure 8. Most cases exceed the desired efficiency target. The single-shaft turbine results in high rotational speeds to maintain high efficiency operation. Thus, split-shaft options were considered to assess alternative means of converging on a design with a reasonable high efficiency operating range. The drive turbine trends shifted to significantly lower speeds. This change is anticipated because the power requirement is approximately one third and pressure ratio half of the single-shaft case. Consider the following equation for specific speed ( $n_s$ )

$$n_s = N \frac{\sqrt{Q_2}}{(\Delta H_s)^{.75}}$$

where  $N$  is the actual rotational speed,  $Q_2$  is the exit volume flow rate and  $\Delta H_s$  is the change in isentropic enthalpy. For a series split-shaft configuration, flow will be the same between the turbines. The series split-shaft configuration requires less power (at the same flow rate) from each turbine compared to the single-shaft configuration; therefore, the change in isentropic head will be less for the split-shaft case. Thus, for a given  $n_s$  which will result in the similar peak efficiency, the split-shaft turbines will operate at a lower speed. Similar to the drive turbine, the power turbine results shift to lower optimal speeds.

This section highlighted turbomachinery design choices which aimed to maximized efficiency with cycle case 2. These high-efficiency configurations (single- and split-shaft) will require many technological risks. These challenges and technology gaps are discussed in detail in the following Component Limits section. Therefore, while maximum efficiency is a desirable design trait, the resulting system may be cost- or risk-prohibited. An alternative solution to the 500 kW sCO<sub>2</sub> cycle would a design which sacrifices some efficiency to allow for the incorporation of more mature technologies. For example, cycle case 6 is a safe (lower technology risk) cycle which uses turbomachinery at lower efficiencies, mainly due to operating at lower speeds. Results from design parameter sweeps for this case are included in the Appendix for reference.

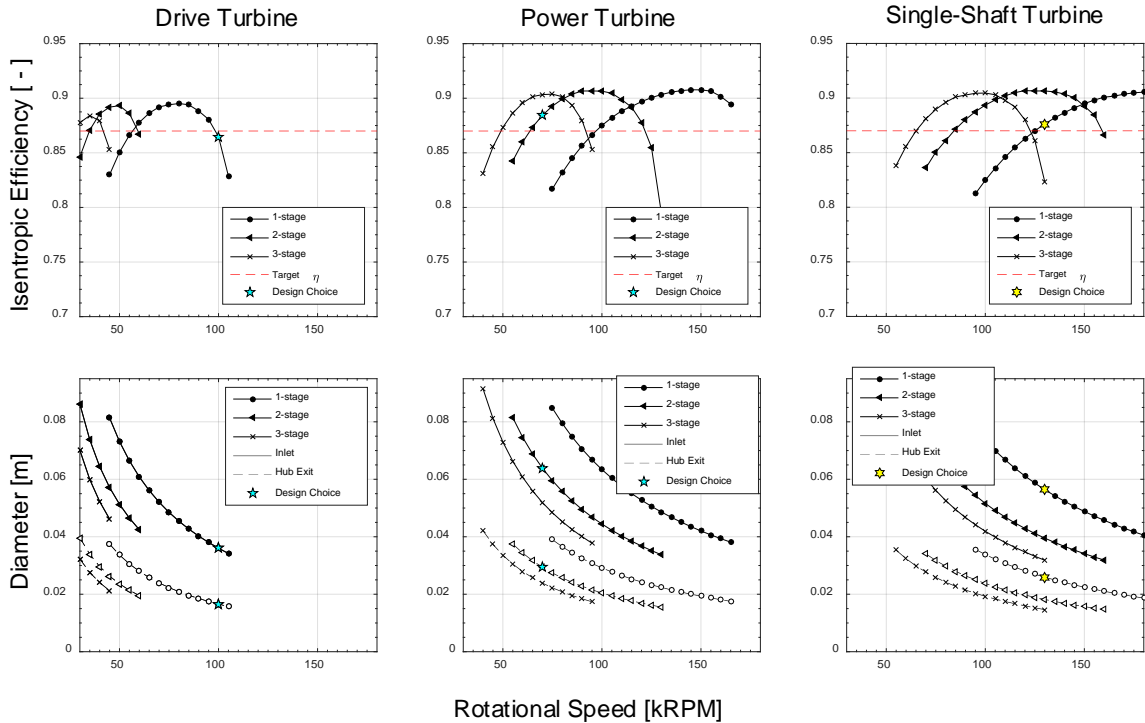


Figure 8. Turbine efficiency and sizing results from design parameter sweeps for Cycle Case 2

## COMPONENT LIMITS

A thorough cycle design process should consider the practical limits of various cycle components that may restrict the aerodynamic sizing and, therefore, ultimate machinery efficiencies that are considered for cycle design. Generally, these components include heat exchangers and various turbomachinery components including bearings, seals, gearboxes, motor/generators, and even the machinery shafts (including rotordynamic limits and shaft stress safety factors). Component limits are highly sensitive to specific component selection and are a complex function of many variables, including speed, load, pressure, temperature, materials, duty cycle, life requirements, etc. However, for purposes of efficiency in the initial cycle design process, the authors will provide general guidelines for near-term component limits based on their experience in designing sCO<sub>2</sub>-based systems.

### Heat Exchangers

sCO<sub>2</sub> cycles are highly recuperated, and heat exchanger effectiveness is a strong driver of cycle efficiency. Although very high-effectiveness heat exchangers can be built, cost constraints on effectiveness values should be considered during sCO<sub>2</sub> cycle evaluation and design. Some cost versus effectiveness guidelines for printed circuit recuperators were presented by Shiferaw et al. [2016], noting that cost increases exponentially at high effectiveness values, resulting in relatively high capital costs for values above about 0.95.

The maximum operating temperature of a heat exchanger is also a strong cost driver for sCO<sub>2</sub> systems. In general, heat exchangers below 600 °C can use relatively low-temperature stainless steel alloys. Higher operating temperatures require nickel alloys, increasing cost by a factor of 2-2.5. Off-design cycle operation should be considered when selecting the heat exchanger design temperature, since the design-point case may not cause the highest temperature.

## Shaft End Seals

For a closed-loop power cycle, minimization of end seal leakage is important to maintaining high cycle efficiency and also reducing CO<sub>2</sub> makeup requirements. Dry gas seals are non-contacting face seals with a rotating ring and stationary ring that minimize leakage via a very small clearance of approximately 3-8 microns. Due to the tight clearance, dry gas seals require an external supply of filtered gas that must also be temperature controlled above 80-100 °C to prevent dry ice formation across the seal and blockage of seal vents. The operating temperature of the seal is also typically limited to ~200-230 °C to avoid failure of a polymer sliding static seal that allows the stationary ring to move with the rotor. A more detailed discussion of dry gas seal and supply system requirements for sCO<sub>2</sub> applications is provided in [Allison et al. 2017 and Allison et al. 2018]. Despite these requirements, dry gas seals are often considered for this purpose due to their extremely low leakage rates and long life. Detailed values for supply flow and temperature requirements as well as expected leakage flow depend on seal geometry details and should be calculated or obtained from a manufacturer.

Commercially available dry gas seals have a maximum operating speed of 50,000-55,000 rpm with maximum shaft diameters of 37.5-35mm, respectively. Larger seals are available at low speeds up to approximately 350mm. Discussions with seal OEMs indicate that custom designs with higher speeds may be possible up to 75,000 rpm, and existing research for sCO<sub>2</sub> applications is focused on improving high-temperature capabilities for turbine dry gas seals.

## Bearings

Bearings can be categorized in four basic groups: rolling element, sliding element, magnetic, and fluid-film. A detailed discussion of bearing types and considerations for sCO<sub>2</sub> applications is provided by Allison et al. [2017] and Brun et al. [2017]. Although various bearing types may be suitable for different sCO<sub>2</sub> applications, this paper focuses primarily on fluid-film oil bearings as they are expected to be the most prevalent. Oil-film bearings are broadly used in many industrial applications and have high durability, high stiffness, and good damping characteristics. Other bearing types may be possible and even favorable for specific small-scale sCO<sub>2</sub> applications, but in general magnetic bearings will be more costly and have lower load capacity and gas bearings may have lower load capacity (hydrodynamic gas foil bearings) or lower damping (hydrostatic gas bearing). In general, the use of gas-film bearings is attractive for sCO<sub>2</sub> turbomachinery but a good understanding of load capacity, damping, and stiffness at sCO<sub>2</sub> conditions is necessary and would likely require dedicated component testing.

Oil-film bearings are available over a variety of speeds and sizes from very large utility-scale machines (e.g., 500 MWe, 3600 rpm) to turbocharger-sized machines operating at 130,000 rpm. A typical limit for oil-film bearings is that the shaft speed must be less than approximately 110 m/s [Nicholas, 2003], although higher surface speeds may be possible. This limit affects the maximum shaft diameter at the bearing locations and must be considered in shaft sizing calculations.

## Motor/Generator

The most economical option for a motor/generator is to use an induction motor/generator with a speed of 1800 or 3600 rpm. These can achieve high power conversion efficiency of 96-98% and are available at all power levels from a variety of vendors worldwide.

For small-scale systems, it may be of interest to consider high-speed motor/generator units to enable high turbomachinery speeds. These high-speed generators are much more costly than their synchronous counterparts and will also incur additional power electronics (with additional losses of 2-5%) to convert the electrical power to line frequency. An experience chart showing speed and power rating of various high-speed motor generators is provided in Figure 9, with a curve fit indicating a maximum power

obtained vs. motor/generator speed. For the 500 kWe example system considered in this paper, a maximum achievable speed is approximately 65,000 rpm depending on conversion losses.

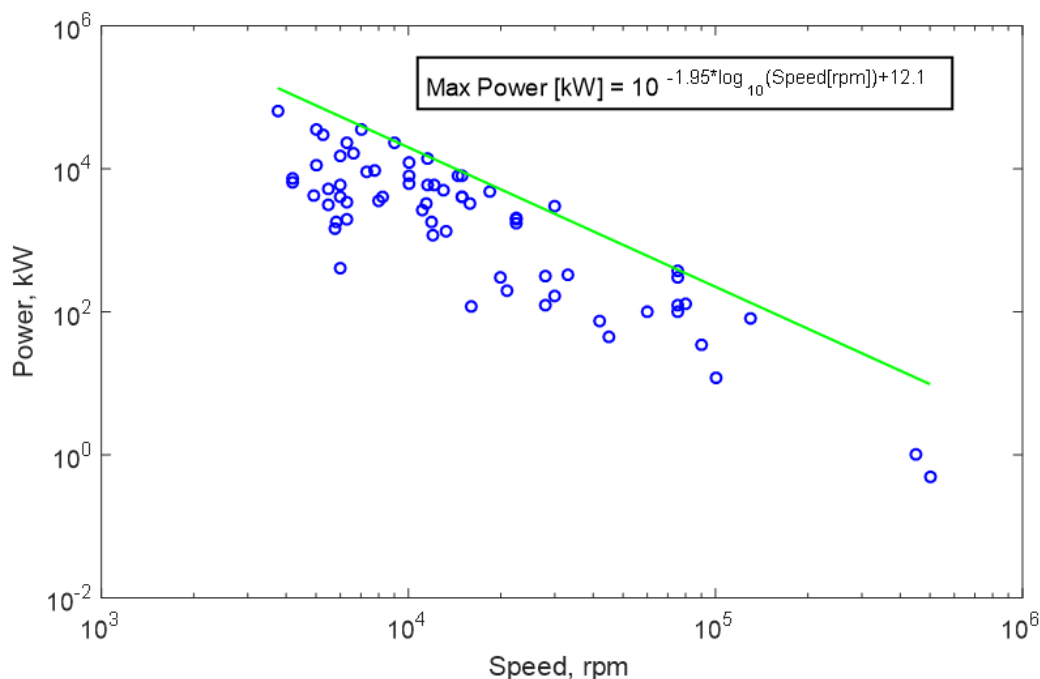


**Figure 9. High-Speed Motor/Generator Experience Chart**

Integral machines include a motor/generator within the pressure casing, eliminating the need for end seals. Previous experience with integral turbine-alternator-compressor units at Sandia National Laboratories and Bettis Atomic Power laboratories highlighted the high windage losses that are expected due to relatively large motor rotors exposed to high-density fluids [Clementoni et al., 2015].

### **Gearbox**

The choice to include a gearbox depends on the scale, efficient turbomachinery speeds, and other layout options including the sealing configuration or single- or dual-shaft configurations. Gearboxes are available at shaft power ratings up to approximately 60 MW [GE Oil & Gas, 2016] and are often considered for coupling the turbine to a synchronous generator at 1800 or 3600 rpm. A gearbox may also be used to separate turbine and compressor speeds. Gearbox losses can reduce the overall system efficiency by 1.5% - 5% depending on scale and operating speeds, but this penalty may be sufficiently offset by improved turbomachinery efficiency at higher speeds.

For small systems in the kWe-scale or low MWe-scale range (such as the 500 kWe system described in this paper), the maximum speed for a single-stage gearbox with a low-speed pinion operating at 3600 rpm is approximately 50,000 rpm. Two-stage or other gearbox configurations can reach higher speeds, but additional complexity will increase cost and transmission losses.

### **Couplings**

sCO<sub>2</sub> turbomachines typically operate with a combination of high power and speed, which may require custom coupling designs for high power applications. However, the literature and authors' experience indicates that coupling designs have been successfully quoted from vendors for various applications ranging from 75000 rpm / 375 kWe to 3600 rpm / 340 MWe. Thus, couplings are not expected to be a limiting technology for sCO<sub>2</sub> turbomachinery designs.

## Shaft

Conceptual shaft layout calculations should be performed during cycle design in order to ensure that aerodynamic sizing and stage counts are adequately balanced by mechanical and rotordynamic considerations when predicting achievable turbomachinery performance. In general, a detailed mechanical design involves an iterative design between rotordynamics, aerodynamics, and mechanical design of the casing as illustrated in Figure 10.

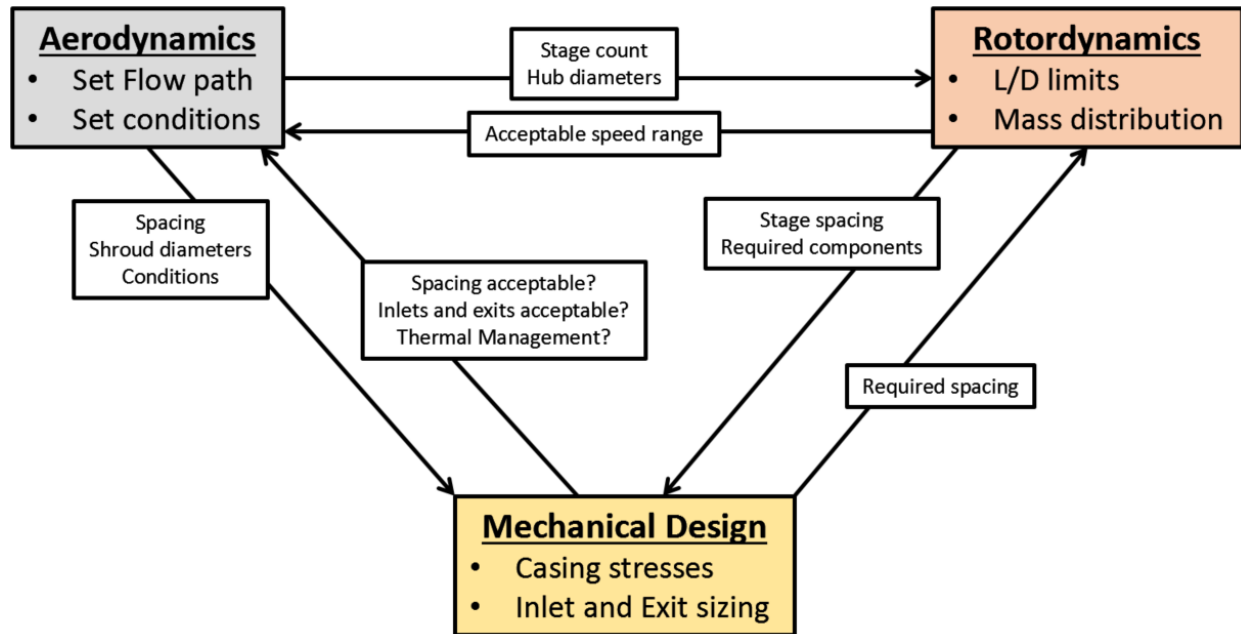


Figure 10. Iterative Design Process for Turbomachinery [Cich, 2018]

For efficiency during a cycle design process, conceptual-level shaft layout considerations are recommended for estimating shaft geometry and rotordynamic limits prior to detailed analysis and design work. For this purpose, conceptual shaft length estimates for aero stages, balance pistons, thermal management features, end seals, and bearings are presented in Table 2. Length estimates are based on radial machinery that is expected at the 500 kWe scale.

The estimated length for aerodynamic components is based on both wheel length and length of stationary flow path components (inlets, exits, diffusers, stator vanes). In later design steps, actual length requirements must be determined from aerodynamic simulation and analysis of the stages. In later design steps, minimum thickness of stationary flow path components must also be considered for structural integrity, but in the authors' experience the required thickness does not affect shaft geometry significantly for the purposes of conceptual length requirements. Another consideration for sCO<sub>2</sub> machinery is that aerodynamic requirements for compressors operating near the critical point are fairly small. For this purpose, it is typically prudent to locate the main compressor stage(s) on the non-drive end of the machine where the reduced shaft diameter is less likely to affect rotordynamics negatively and the transmitted torque is small.

Where back-to-back stages exist, a division wall seal is necessary to isolate the stages from each other. The actual length requirement will depend on the allowable leakage and differential pressure between the adjacent flow paths, but a conceptual estimate is provided in Table 2. Division wall seal leakage is highly dependent on the seal type (often a labyrinth seal) and pressure differential of neighboring stages.

If pressures are significantly different, the impact of division wall leakage should be included in estimated machinery efficiencies.

The balance piston is sized to minimize rotor thrust under nominal conditions and for single-shaft machines will typically be located to experience the full machine pressure differential (the cavity downstream of the seal is connected to the low-pressure piping). If this is placed near the shaft end, then this also causes the sealing pressure of both end seals to be matched. In detailed design the balance piston length will be finalized to minimize leakage (longer seal) and, for sCO<sub>2</sub> machines, is likely to be a damper seal (e.g., hole pattern or honeycomb) for enhancing rotordynamic stability. The balance piston leakage is typically not insignificant and should be included in estimated machinery efficiencies.

For sCO<sub>2</sub> turbines, a thermal management region will be required between the turbine stages and low-temperature seals (e.g., dry gas seals) or bearings. The purpose of this region is to control the thermal gradient along the shaft and casing so that it is predominantly axial, thus minimizing stress. The features for controlling the thermal gradient are typically proprietary design information, but a rule of thumb for conceptual rotor length estimations is provided in Table 2 based on an example turbine design in [Brun et al., 2017] and scaling of published turbine design images.

Dry gas seal length depends on the seal configuration (single, tandem, etc.) and corresponding separation seal (isolates the dry gas seal from bearing oil). sCO<sub>2</sub> is an inert fluid, so a single-seal configuration is typically considered to be sufficient and minimizes shaft length. The length and diameter estimates shown in Table 2 are based on various vendor quotes for multiple applications, although designs can vary significantly among vendors and later design efforts should include final dimensions provided by an OEM.

Finally, the estimated lengths for bearings presented in Table 2 are approximations for oil-film bearings and actual dimensions may vary depending on required load capacity, stiffness, damping, etc.

**Table 2. Shaft Component Length and Diameter Estimates**

<b>Component</b>	<b>Shaft Length Estimate</b>	<b>Shaft Diameter Estimate</b>
Aero Stage	1-1.2 tip diameters (radial)	From aero sizing hub diameter
Division Wall	0.5 hub diameters	From aero sizing hub diameter
Balance Piston	0.5 piston diameter	Average eye diameter from aero stages
Thermal Management	0.3-0.4 shaft diameters per 100 °C temperature difference	Match with other shaft components
Dry Gas Seal	0.4-1.5 shaft diameters (longer for smaller seals)	Assume from aero hub diameter
Journal Bearings	1.0 shaft diameters	Minimum of aero hub diameter or diameter for 110 m/s surface speed
Thrust Bearing Disk	0.2-0.3x disk diameter	1.2x Average aero tip diameter

After all component lengths have been estimated, it is possible to estimate the shaft safety factors for yield/creep as well as conceptual rotordynamic feasibility. The nominal torsional stress can be calculated for various shaft sections based on the diameter and transmitted power through each section. Low-temperature shafting should have a conceptual safety factor  $\geq 5.0$  to account for non-torsional static loads and lateral/torsional dynamic loading. High-temperature shaft sections should be evaluated for creep based on the desired life and a minimum safety factor of 1.5. The yield and creep strength for these sections will depend on the temperature and material choice.

Generally, sCO<sub>2</sub> machinery rotordynamics are a limiting factor before yield/creep issues become significant. The bearing span and average shaft diameter from conceptual layout values can be used to calculate an overall L/D ratio for the machine for a conceptual-level rotordynamics screening. Final rotordynamic acceptability must be determined with a detailed API 617 [API, 2014] rotordynamic analysis including calculation of destabilizing cross-coupling forces in impellers and seals (the high density of sCO<sub>2</sub> increases the risk of rotordynamic instability due to these cross-coupling forces). For conceptual purposes a maximum L/D of 9-12 is recommended by Cich [2018].

## MECHANICAL SYSTEM LAYOUTS

This section presents several potential system layouts for the example 500 kWe sCO<sub>2</sub> cycle. The layouts were selected based on the aerodynamic sizing results and conceptual-level shaft layout calculations that consider the various component limits described in the previous section. The aerodynamic sizing results can be used to quickly highlight stage counts and speeds that are expected to provide high efficiencies and speed matching between machinery components. The results show that, at this scale, the attainment of high compressor aerodynamic efficiencies at low stage counts is likely to require high operating speeds at or above 100,000 rpm.

The first conceptual layout prioritizes high efficiency and minimum stage count by maximizing operating and packing all elements in a single body. The resulting unit is shown in Figure 11, with an operating speed of 130,000 rpm and single-stage turbine, main compressor, and bypass compressor. The arrangement assumes the existence of a high-speed motor/generator and dry gas seal that are outside the currently available component limits described previously in this paper, but is useful for educational purposes.

The estimated performance and shaft geometry of the unit is summarized in Table 3. Because the estimated turbine and compressor efficiencies are very close to those assumed in cycle iteration 2, values from sizing results for this cycle were used for efficiency and stage geometry. The shaft at the drive-end bearing is required to neck down to 16mm in order to satisfy maximum surface speed requirements, and at this diameter a yield safety factor of 6.0 is achieved (very close to the minimum acceptable value). The approximate L/D for the rotor is 14.9, which is relatively high above the recommended value of 12.0. Thus, the machine will likely require shortening of various shaft elements during detailed design pending rotordynamic analysis results. Because the machine requires nonexistent end seals, it is possible that shaft length could be reduced through the use of immersed gas film bearings, but those components also require validation. An immersed motor/generator is also likely to cause high losses even if the power/speed combination could be achieved.

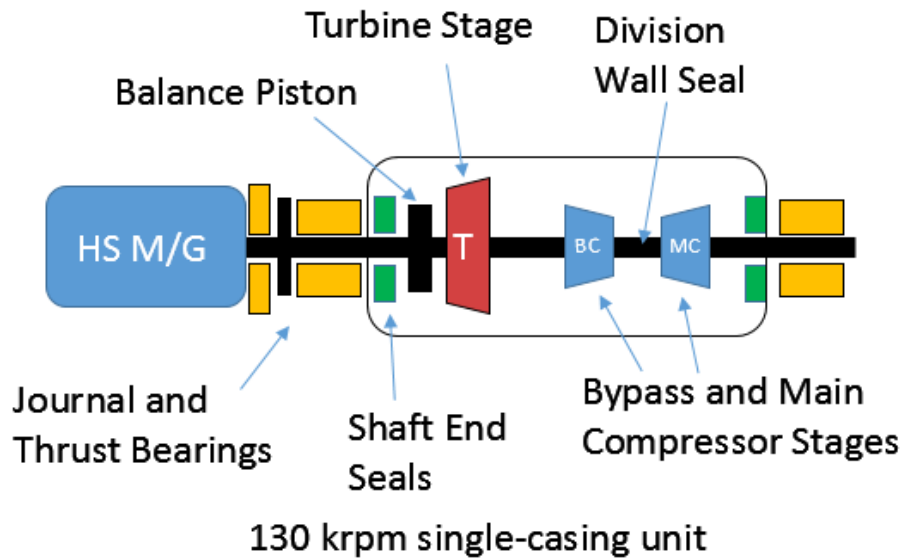


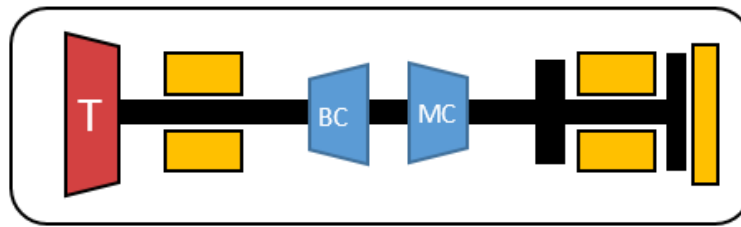
Figure 11. Layout 1 for 500 kWe Cycle

Table 3. Conceptual Performance and Shaft Characteristics of Layout 1

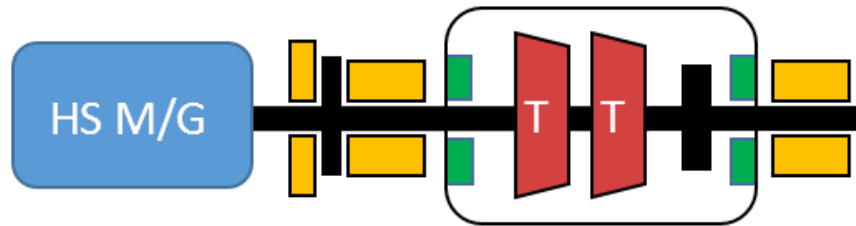
Component	Units	
Main Compressor Efficiency	-	0.79
Bypass Compressor Efficiency	-	0.73
Turbine Efficiency	-	0.88
Main Compressor Hub Diameter	mm	17
Bypass Compressor Hub Diameter	mm	20
Turbine Hub Diameter	mm	26
Bearing Span	mm	332
Bearing Surface Speed	m/s	109
L/D	-	14.9
Min Yield Safety Factor	-	6.0 (at DE bearing)
Min Creep Safety Factor	-	4.6 (at turbine)

Due to the problems with Layout 1, a second split-shaft layout (see Figure 12) is considered that utilizes an immersed turbo-compressor and separate lower-speed motor-generator. The immersed turbo-compressor does require immersed bearings, which may be achievable although some component development and validation testing will likely be necessary.

The conceptual performance and shaft sizing results for the units are summarized in Table 4. The estimated efficiencies fall between cycle iterations 1 and 3, average values from sizing results corresponding to both of these cycles were used for efficiency and stage geometry (the results are similar for both cycles). In general, this configuration satisfies rotor constraints for both machines. The overhung turbine and thrust bearing in the turbo-compressor reduce the L/D considerably. The turbo-generator's L/D is marginal, but a solution is likely achievable during detailed design. Safety factors for yield and creep are also very high.



100 krpm turbo-compressor



55 krpm turbo-generator

Figure 12. Layout 2 for 500 kWe Cycle

Table 4. Conceptual Performance and Shaft Characteristics of Layout 2

Component	Units	Turbo-Compressor	Turbo-Generator
Main Compressor Efficiency	-	0.77	-
Bypass Compressor Efficiency	-	0.68	-
Turbine Efficiency	-	0.88	0.85
Main Compressor Hub Diameter	mm	21	-
Bypass Compressor Hub Diameter	mm	20	-
Turbine Hub Diameter	mm	20	37
Bearing Span	mm	212	413
Bearing Surface Speed	m/s	99	104
L/D	-	10.5	11.2
Min Yield Safety Factor	-	18 (at turbine)	24.5 (at turbine)
Min Creep Safety Factor	-	4.1 (at turbine)	5.6 (at turbine)

Finally, a third machinery layout is presented in Figure 13 that minimizes risk by reducing speed to utilize existing commercially available components, though at the cost of reduced efficiency compared to the previous two layouts. This layout increases stage count for the turbine and re-compressor in order to boost efficiency, but separates the units into separate casings to reduce L/D. A gearbox is shown to a low-speed motor/generator, but a high-speed motor/generator is likely a viable alternative option to consider.

The conceptual performance and shaft sizing results for this low-speed layout are summarized in Table 5. Although 3 stages are shown in Figure 13, both two- and three-stage turbines are considered in the table to illustrate the mechanical design tradeoffs. Aero sizing results corresponding to cycle iteration 4 were used because of the close match in machinery efficiencies. The results show easily achievable surface speeds and excellent yield/creep safety factors, but marginal L/D for the compressor unit and 3-stage

turbine unit due to the relatively high stage count. This L/D can likely be reduced some during detailed design if detailed rotordynamic analysis results indicate that it is necessary.

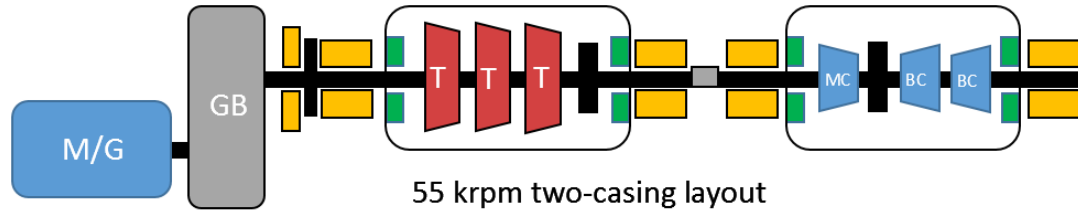


Figure 13. Layout 3 for 500 kWe Cycle

Table 5. Conceptual Performance and Shaft Characteristics of Layout 3

Component	Units	Compressor Unit	Turbine Unit (2-stage)	Turbine Unit (3-stage)
Main Compressor Efficiency	-	0.67	-	-
Bypass Compressor Efficiency	-	0.65	-	-
Turbine Efficiency	-	-	0.81	0.86
Main Compressor Hub Diameter	mm	21	-	-
Bypass Compressor Hub Diameter	mm	26	-	-
Turbine Hub Diameter	mm	-	42	34
Bearing Span	mm	316	447	455
Bearing Surface Speed	m/s	67	95	95
L/D	-	13.0	10.7	13.5
Min Yield Safety Factor	-	16.7 (at DE bearing)	17.4 (at GB side bearing)	17.4 (at GB side bearing)
Min Creep Safety Factor	-	-	8.1 (at turbine)	4.3 (at turbine)

## SUMMARY

The conceptual design process for a notional 500 kW sCO<sub>2</sub> power block has been presented highlighting the interactions between thermodynamic cycle design, aerodynamic design, and mechanical system layout. Trades in the aerodynamic design of the Main Compressor, Bypass Compressor, and Turbine combined experience based mechanical system limitations led to the development of three system concepts which represent a high risk, high speed, high efficiency single shaft machinery layout, a lower risk, high speed split shaft machinery layout, and a low risk, low efficiency system layout using conventional components. The developed system layouts highlight several of the technology gaps in seals, bearings, and generators that have a significant impact on the design of high efficiency kW scale sCO<sub>2</sub> systems.

## REFERENCES

Allison, T., Moore, J.J., Wilkes, J.C., and Brun, K. (2017). "Turbomachinery Overview for Supercritical CO<sub>2</sub> Power Cycles." *Proc 46<sup>th</sup> Turbomachinery Symposium*, Houston, Texas.

Allison, T., Moore, J.J., Day, M., Hofer, D., and Thorp, J. (2018). "Planning for Successful Transients and Trips in a 1 MWe-Scale High-Temperature sCO<sub>2</sub> Test Loop." *Proc. ASME Turbo Expo GT2018-75873 (accepted for publication)*, Oslo, Norway.

American Petroleum Institute (2014). "Axial and Centrifugal Compressors and Expander-Compressors for Petroleum." *API Standard 617 8<sup>th</sup> Ed.*, Chemical and Gas Industry Services, Washington, D.C.

Aungier, R. H., 2000, *Centrifugal Compressors: A Strategy for Aerodynamic Design and Analysis*, ASME Press.

Balje, O. E., 1981, *Turbomachines: A Guide to Design Selection and Theory*, John Wiley & Sons, New York.

Bidkar, R.A., Musgrove, G., Day, M., Kulhanek, C.D., Allison, T., Peter, A., Hofer, D., and Moore, J., 2016, "Conceptual Designs of 50MWe and 450MWe Supercritical CO<sub>2</sub> Turbomachinery Trains for Power Generation from Coal. Part 2: Compressors." Proceedings of the 5th International Symposium - Supercritical CO<sub>2</sub> Power Cycles, San Antonio, Texas.

Brun, K., Friedman, P., and Dennis, R.. "Fundamentals and Applications of Supercritical Carbon Dioxide (sCO<sub>2</sub>) Based Power Cycles." Woodhead Publishing, 2017.

Cich, S. (2018). "2D Machinery Layouts." *SwRI Turbomachinery Design Training Week*, San Antonio, Texas.

Clementoni, E.M., Cox, T.L., and King, M.A. (2015). "Off-Nominal Component Performance in a Supercritical Carbon Dioxide Brayton Cycle." *Proc. ASME Turbo Expo GT2015-42501*, Montreal, Canada.

Lemmon, E. W., Huber, M. L., and McLinden, M. O., 2013. "NIST Standard Reference Database 23: Reference Fluid Thermodynamic and Transport Properties—REFPROP." Version 9.1, National Institute of Standards and Technology, Standard Reference Data Program, Gaithersburg, Maryland.

GE Oil & Gas (2016), Gearbox Technology. Available from: <https://www.geoilandgas.com/liquefied-natural-gas/gas-liquefaction/gearbox-technology> [Accessed 16 May 2016].

NASA. "RTD Radial-Inflow Turbine Conceptual Design Code." Reference Number LEW-17453-1, <https://software.nasa.gov/software/LEW-17453-1>.

Nicholas, J. (2003). "Tilting Pad Journal Bearings with Spray-Bar Blockers and By-Pass Cooling for High Speed, High Load Applications." *Proc. 32<sup>nd</sup> Turbomachinery Symposium*, Houston, Texas.

Rohlik, 1968. "Analytical Determination of Radial Inflow Turbine Design Geometry for Maximum Efficiency." NASA TN D-4384.

APPENDIX

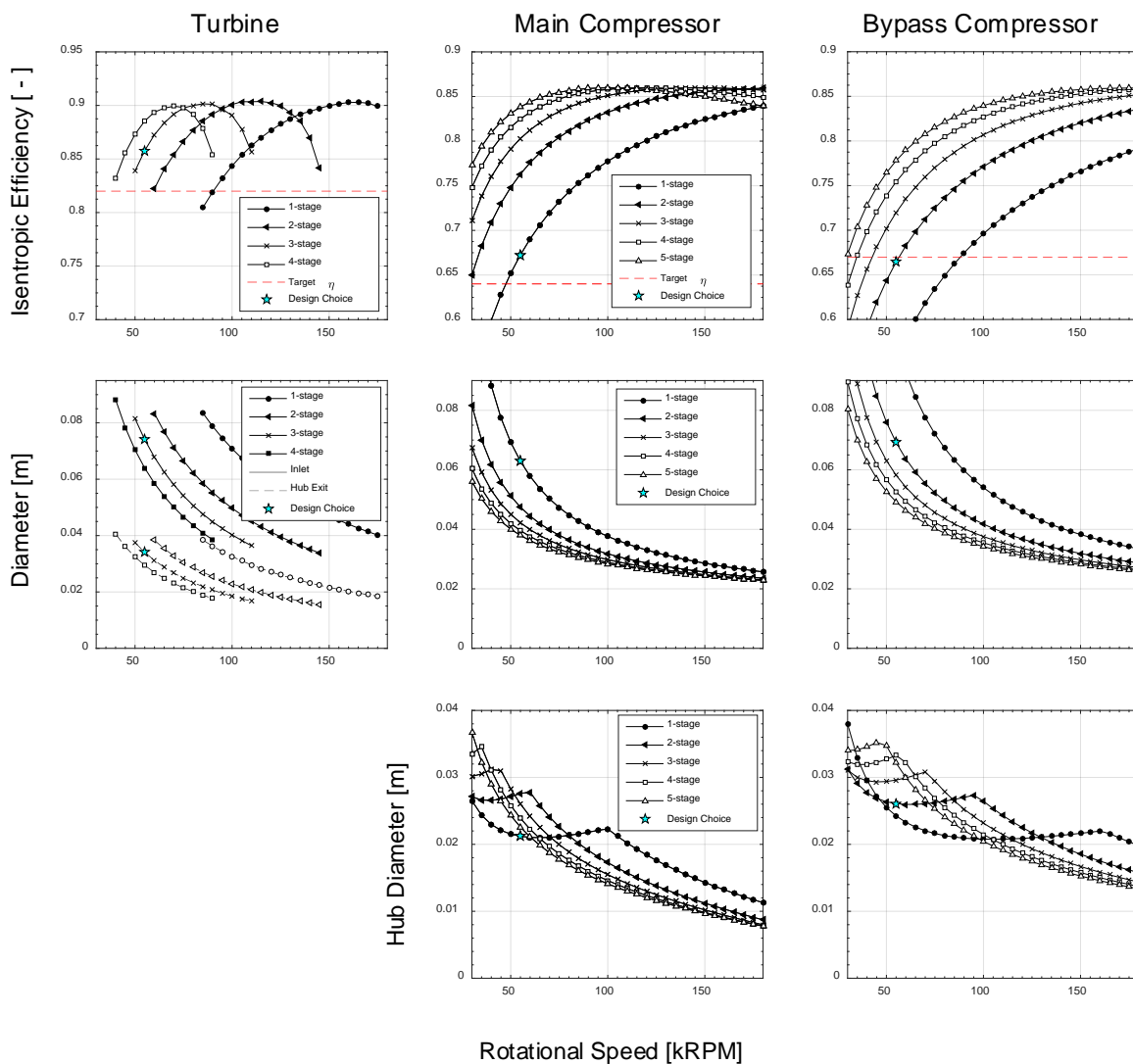


Figure 14. Turbine, compressor, and bypass compressor efficiency and sizing results from design parameter sweeps for Cycle Case 6